


# Long Noncoding RNA PCED1B-AS1 Promotes the Warburg Effect and Tumorigenesis by Upregulating HIF-1 $\alpha$ in Glioblastoma

Cell Transplantation  
Volume 29: 1–11  
© The Author(s) 2020  
Article reuse guidelines:  
sagepub.com/journals-permissions  
DOI: 10.1177/0963689720906777  
journals.sagepub.com/home/ctj  


Zhiqiang Yao<sup>1</sup>, Qiansheng Zhang<sup>2</sup>, Fuyou Guo<sup>3</sup>, Shewei Guo<sup>3</sup>,  
Bo Yang<sup>3</sup>, Binghui Liu<sup>1</sup>, Panxing Li<sup>1</sup>, Jinyi Li<sup>1</sup>, Sheng Guan<sup>1</sup>,  
and Xianzhi Liu<sup>3</sup> 

## Abstract

Accumulating evidence suggests that long noncoding RNA (lncRNA) functions as a critical regulator in cancer biology. Here, we characterized the role of lncRNA PCED1B antisense RNA 1 (PCED1B-AS1) in glioblastoma (GBM). PCED1B-AS1 was notably upregulated in GBM tissues and cell lines and closely associated with larger tumor size and higher grade. Patients with high PCED1B-AS1 had shorter survival time than those with low PCED1B-AS1. Functional experiments showed that depletion of PCED1B-AS1 significantly inhibited, while overexpression of PCED1B-AS1 promoted cell proliferation, glucose uptake, and lactate release. Mechanistically, PCED1B-AS1 was able to directly bind to the 5'-UTR of HIF-1 $\alpha$  mRNA and potentiate HIF-1 $\alpha$  translation, leading to increased HIF-1 $\alpha$  protein level, thereby promoting the Warburg effect and tumorigenesis. Importantly, PCED1B-AS1 lost the carcinogenic properties in the absence of HIF-1 $\alpha$ . In addition, we also confirmed the existence of the PCED1B-AS1/HIF-1 $\alpha$  regulatory axis *in vivo*. Taken together, our findings demonstrate that PCED1B-AS1 is a novel oncogenic lncRNA in GBM and functions in a HIF-1 $\alpha$ -dependent manner, which provides a promising prognostic biomarker and drug-gable target for GBM.

## Keywords

long noncoding RNA, Warburg effect, biomarker, translation, tumorigenesis

## Introduction

Glioblastoma (GBM) is the most common and fatal malignant primary brain tumor in adults, accounting for 12% to 15% of all intracranial tumors and 50% to 60% of astrocytic tumors<sup>1</sup>. It is able to rapidly invade and infiltrate normal peripheral brain tissue, making complete resection impossible<sup>2</sup>. Therefore, the standard treatment at present is surgery combined with radiotherapy and chemotherapy<sup>3</sup>. The 5-year survival rate of patients with GBM is very unfavorable, less than 5%, and this indicator drops to 2% among patients aged 65 years or older<sup>4</sup>. A better understanding of the pathogenesis of GBM will provide new approaches for treatment and improve the outcomes of patients.

The occurrence and progression of cancer is an extremely complex process, accompanied by a variety of pathophysiological changes. Emerging evidence suggests that abnormal glucose metabolism is a hallmark of cancer<sup>5</sup>. In normal cells, the final product of glucose can be lactic acid, or it can be

<sup>1</sup> Department of Interventional Neuroradiology, The First Affiliated Hospital of Zhengzhou University, Henan, China

<sup>2</sup> Department of Neurosurgery, The First Affiliated Hospital and College of Clinical Medicine of Henan University of Science and Technology, Luoyang, Henan, China

<sup>3</sup> Department of Neurosurgery, The First Affiliated Hospital of Zhengzhou University, Henan, China

Submitted: September 16, 2019. Revised: October 20, 2019. Accepted: January 15, 2020.

### Corresponding Authors:

Xianzhi Liu, Department of Neurosurgery, The First Affiliated Hospital of Zhengzhou University, 1 Jianshe Road, Zhengzhou 450052, Henan, China.

Email: liuxz85@yeah.net;

Sheng Guan, MD, Department of Interventional Neuroradiology, The First Affiliated Hospital of Zhengzhou University, 1 Jianshe Road, Zhengzhou 450052, China.

Email: guanszz6@126.com



Creative Commons Non Commercial CC BY-NC: This article is distributed under the terms of the Creative Commons Attribution-NonCommercial 4.0 License (<https://creativecommons.org/licenses/by-nc/4.0/>) which permits non-commercial use, reproduction and distribution of the work without further permission provided the original work is attributed as specified on the SAGE and Open Access pages (<https://us.sagepub.com/en-us/nam/open-access-at-sage>).

**Table 1.** Correlation Between PCED1B-AS1 Expression and Clinicopathological Features in GBM Patients ( $n = 76$ ).

Parameters	All cases	PCED1B-AS1 expression		P value
		Low ( $n = 38$ )	High ( $n = 38$ )	
Gender				
Male	42	22	20	0.645
Female	34	16	18	
Age (years)				
$\leq 50$	37	21	16	0.251
$> 50$	39	17	22	
Tumor size (cm)				
$\leq 5$	31	23	8	$< 0.001$
$> 5$	45	15	30	
Histological subtype				
IDH1 wild	62	33	29	0.237
IDH1 mutant	14	5	9	
Pathological grade				
I-II	36	24	12	0.006
III-IV	40	14	26	

GBM: glioblastoma; PCED1B-AS1: PCED1B antisense RNA 1.

completely oxidized by respiration in the mitochondria to produce  $\text{CO}_2$ , depending on the oxygen content<sup>6</sup>. Cancer cells, however, prefer glycolysis, even under aerobic conditions, leading to dramatically increasing glucose uptake and lactate production, a phenomenon known as aerobic glycolysis, also called the Warburg effect<sup>7</sup>. Enhanced Warburg effect helps cancer cells to minimize oxidative stress, thereby promoting tumorigenesis and aggressive progression<sup>8</sup>.

Long noncoding RNA (lncRNA) is a class of endogenous noncoding RNA longer than 200 nt in length. Multiple lines of evidence show that lncRNA functions as a pivotal regulator in the Warburg effect. For example, lincRNA-p21<sup>9</sup>, IDH1-AS1<sup>10</sup>, and MALAT1<sup>11</sup> were proposed to govern the Warburg effect through regulating some key oncogenes, such as c-Myc and HIF-1 $\alpha$ . In this study, we identified a glycolysis-related lncRNA, PCED1B antisense RNA 1 (PCED1B-AS1), which was remarkably elevated in GBM tissues and cell lines. Furthermore, the underlying mechanism by which it facilitated the Warburg effect and tumorigenesis was also deciphered.

## Materials and Methods

### GBM Tissues and Cell Lines

We collected 76 pairs of primary GBM and adjacent normal tissues from The First Affiliated Hospital of Zhengzhou University. All specimens were histologically confirmed by two independent experienced pathologists. The detailed clinical information of patients is summarized in Table 1. Patients were followed up with routinely after surgery, and each patient provided informed consent. This study was approved by the Ethics Committee of The First Affiliated Hospital of

**Table 2.** The Primer Sequences Used in This Study.

Gene	Direction	Sequence (5'-3')
PCED1B-AS1	Forward	TCAAGCCAATCAGCTGACAC
	Reverse	AAACAAATGCCCTGCTTGAC
HIF-1 $\alpha$	Forward	CCAGATCTCGGCGAAGTAAA
	Reverse	CCTCACACGCAAATAGCTGA
UI	Forward	GTGGTTTTTCCAGAGCAAGG
	Reverse	CAGGGGAAAACACAGACACA
GAPDH	Forward	ACCCAGAAGACTGTGGATGG
	Reverse	TTCAGCTCAGGGATGACCTT
EGRI	Forward	CTGCACGTTTCTCAGTGTTT
	Reverse	GATCCGAACGGGTCAGAGAT
ANGPTL4	Forward	ACTCTAGAGGCGTGGACCAA
	Reverse	TACACACAACAGCACCAGCA
IGFBP3	Forward	GCCTGGATTCCACAGCTTC
	Reverse	GAGCAGCACCAGCAGAGTC
PKM2	Forward	GAAGGGTGTGAACCTTCCTG
	Reverse	CTTCTCTCCCAGGACCTTCC
LDHA	Forward	TGGCTGTCTCTTGTGTAG
	Reverse	AGCGTGGAAAAGGAATATCG

Zhengzhou University. A total of six GBM cell lines (U87MG, U251MG, SHG44, Ln229, T98, and A172) and one normal human astrocyte cell line NHA were obtained from Chinese Academy of Sciences (Shanghai, China) and cultured in Dulbecco's Modified Eagle's Medium (DMEM) (Gibco, Invitrogen, Carlsbad, CA, USA) complete medium containing 10% fetal bovine serum (FBS) (Gibco, Invitrogen, Carlsbad, CA, USA), penicillin, and streptomycin.

### Quantitative Reverse Transcription PCR Analysis

GBM cells and tissues were treated with Trizol reagent (Invitrogen, Carlsbad, CA, USA), followed by extraction by chloroform, precipitation by isopropanol, and dissolution by diethyl pyrocarbonate water. Then, 1  $\mu\text{g}$  RNA was reverse transcribed into cDNA using Molony Murine Leukemia Virus (MMLV) transcriptase (Promega, Madison, WI, USA). Lastly, qPCR was performed using SYBR Green SuperMix (Roche, Basel, Switzerland) on a CFX96 real-time PCR detection system (Bio-Rad, Richmond, CA, USA). The  $2^{-\Delta\Delta C_t}$  method was employed to calculate RNA expression and the results were normalized to glyceraldehyde-3-phosphate dehydrogenase (GAPDH) (Table 2).

### Cell Transfection and Generation of Stably Engineered Cell Lines

Cell transfection was performed using Lipofectamine 3000 reagent (Invitrogen) according to the manufacturer's instructions. To generate stable PCED1B-AS1-depleted (sh-RNA#1: 5'-GGCCUGAAAUACAUUUAAA-3'; sh-RNA#1: 5'-GGUGACUCAUGCCUAUAAU-3') or overexpressed GBM cells, the pCDH-CMV-MCS-EF1-copRFP lentiviral vector was used and infected into cells in the presence of

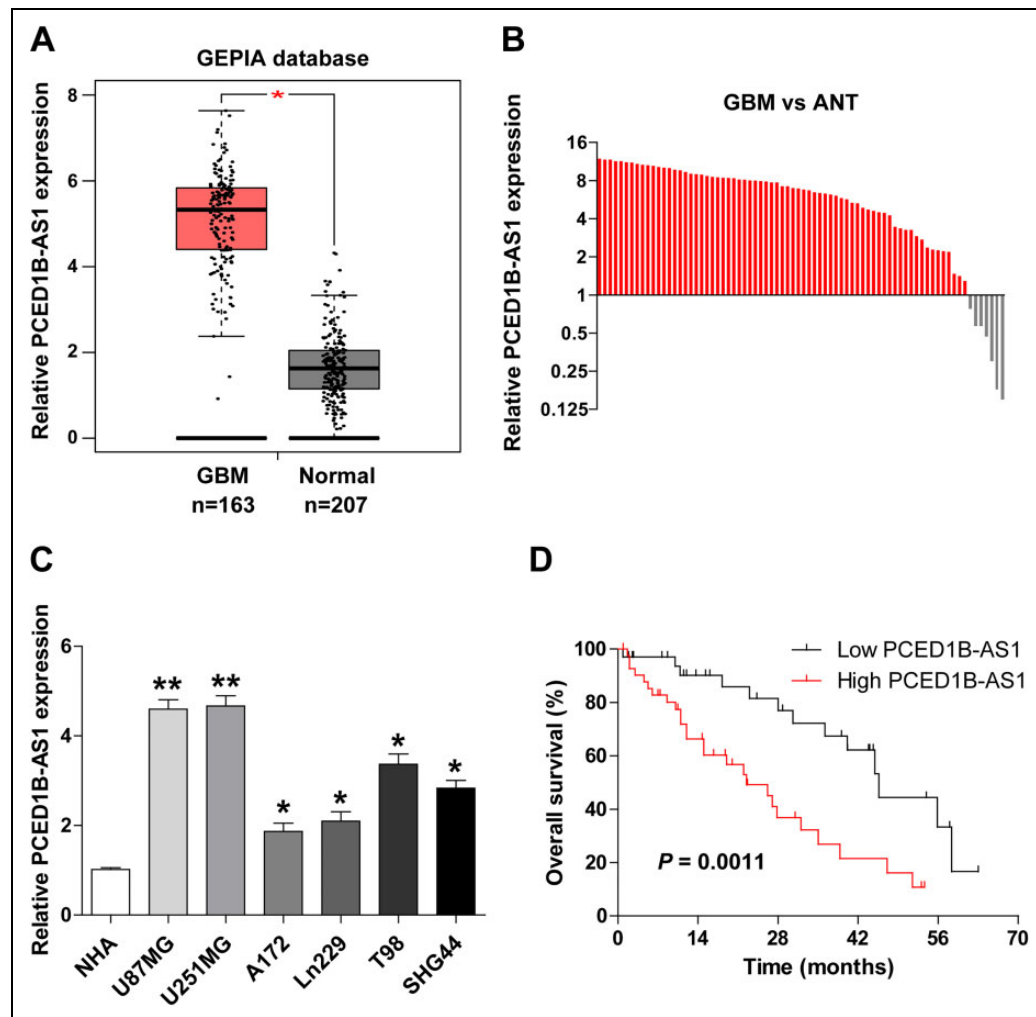


**Fig. 1.** PCED1B-AS1 is frequently overexpressed in GBM. (A) The relative expression of PCED1B-AS1 in GEPIA database. (B) qRT-PCR analysis of PCED1B-AS1 expression in 76 GBM and adjacent normal tissues. (C) qRT-PCR analysis of PCED1B-AS1 expression in GBM cell lines. (D) The survival curve of GBM patients with low or high PCED1B-AS1 based on median PCED1B-AS1 value in 76 GBM tissues. \* $P < 0.05$ , \*\* $P < 0.01$ . ANT: adjacent normal tissue; GBM: glioblastoma; GEPIA: Gene Expression Profiling Interactive Analysis; PCED1B-AS1: PCED1B antisense RNA 1; qRT-PCR: quantitative reverse transcription polymerase chain reaction.

8  $\mu\text{g/ml}$  polybrene. Then, the stable cell lines were selected using puromycin for 2 wk.

#### Cell Counting Kit-8 (CCK-8) and EdU (5-ethynyl-2'-deoxyuridine) Assays

For CCK-8 assay, GBM cells were plated on 96-well plates and grown for 24, 48, and 72 h, followed by treatment with 10  $\mu\text{l}$  CCK-8 solution (Dojindo, Kumamoto, Japan) for 3.5 h at 37°C. Then, the absorbance value at 450 nm in each well was recorded with a microplate reader. For EdU assay, the Cell-Light EdU Apollo488 *In Vitro* Kit (RiboBio, Guangzhou, China) was used as per the manufacturer's protocols and the results were photographed and analyzed by a fluorescence microscope (Olympus, Tokyo, Japan) and Image J software (National Institutes of Health, Bethesda, MD, USA).

#### Glucose Consumption and Lactate Production

The analysis of glucose consumption and lactate production was carried out using Glucose Assay Kit (ab65333, Abcam, Cambridge, UK) and Lactate Assay Kit (ab65330, Abcam) based on the manufacturer's instructions. The absorbance at 570 nm was detected using a microplate reader.

#### Western Blot and Immunohistochemistry (IHC)

Total protein was extracted using lysis buffer supplemented with protease and phosphatase inhibitors. Then, the protein was loaded in SDS-PAGE gel, transferred onto polyvinylidene fluoride (PVDF) member, and blocked by 5% skimmed milk. Finally, the member was incubated with corresponding primary and secondary antibodies and exposed using immobilon western chemiluminescent HRP

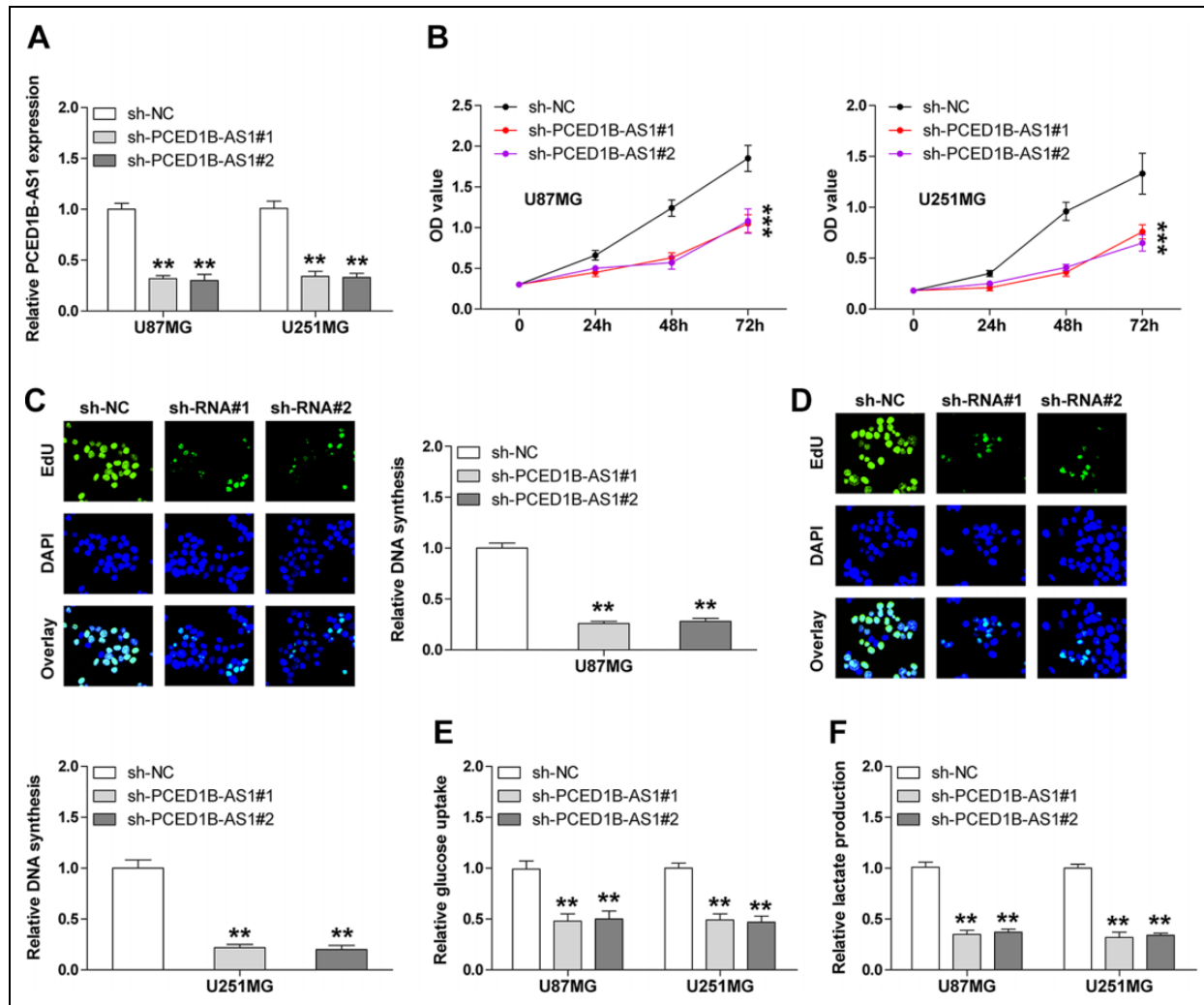


**Fig. 2.** PCED1B-ASI knockdown inhibits GBM cell proliferation, glucose uptake, and lactate release. (A) qRT-PCR analysis for verification of PCED1B-ASI knockdown in U87MG and U251MG cell lines. (B) Cell viability in PCED1B-ASI-depleted U87MG and U251MG cell lines tested by CCK-8 assay. (C and D) DNA synthesis rate in PCED1B-ASI-depleted U87MG and U251MG cell lines detected by EdU assay. (E and F) The levels of glucose uptake and lactate release in U87MG and U251MG cell lines with or without stable PCED1B-ASI knockdown.  $**P < 0.01$ ,  $***P < 0.001$ . EdU: 5-Ethynyl-2'-deoxyuridine; DAPI: 4',6-diamidino-2-phenylindole; GBM: glioblastoma; OD: optical density; PCED1B-ASI: PCED1B antisense RNA 1; qRT-PCR: quantitative reverse transcription polymerase chain reaction.

substrate (Millipore, Schwalbach, Germany). The primary antibodies used in this study are as follows: anti-HIF-1 $\alpha$  (#ab16066, Abcam), anti-c-Myc (#ab32072, Abcam), and anti- $\beta$ -actin (#ab8226, Abcam). For IHC staining, GBM tissues were fixed and embedded into tissue microarray in the Department of Pathology. Then, the paraffin-embedded sections were dewaxed and rehydrated, followed by antigen retrieval, blockade, and incubation with anti-HIF-1 $\alpha$  (#ab16066, Abcam) antibody at 4°C overnight. After incubation with ready-to-use DAKO secondary antibody for 1 h at room temperature, the sections were visualized using diaminobenzidine reagent. The results were analyzed with an optical microscope in 10 random fields by using H-score method<sup>12</sup>.

### Assessment of Translation Level

For polysome profile analysis, the lysates of U87MG and U251MG cells were collected with polysome lysis buffer and loaded onto different sucrose density gradients. After high-speed centrifugation, the RNA in polysome fraction was isolated using Trizol reagent and the expression of HIF-1 $\alpha$  mRNA was detected by quantitative reverse transcription PCR (qRT-PCR). For the luciferase reporter assay, the HIF-1 $\alpha$  5'-UTR containing PCED1B-AS1 binding site was embedded into bicistronic reporter vector; then, the reporter was transfected into stable PCED1B-AS1-depleted U87MG and U251MG cells for 48 h. Finally, the luciferase activity was recorded using dual luciferase reporter system (Promega). For detecting newly

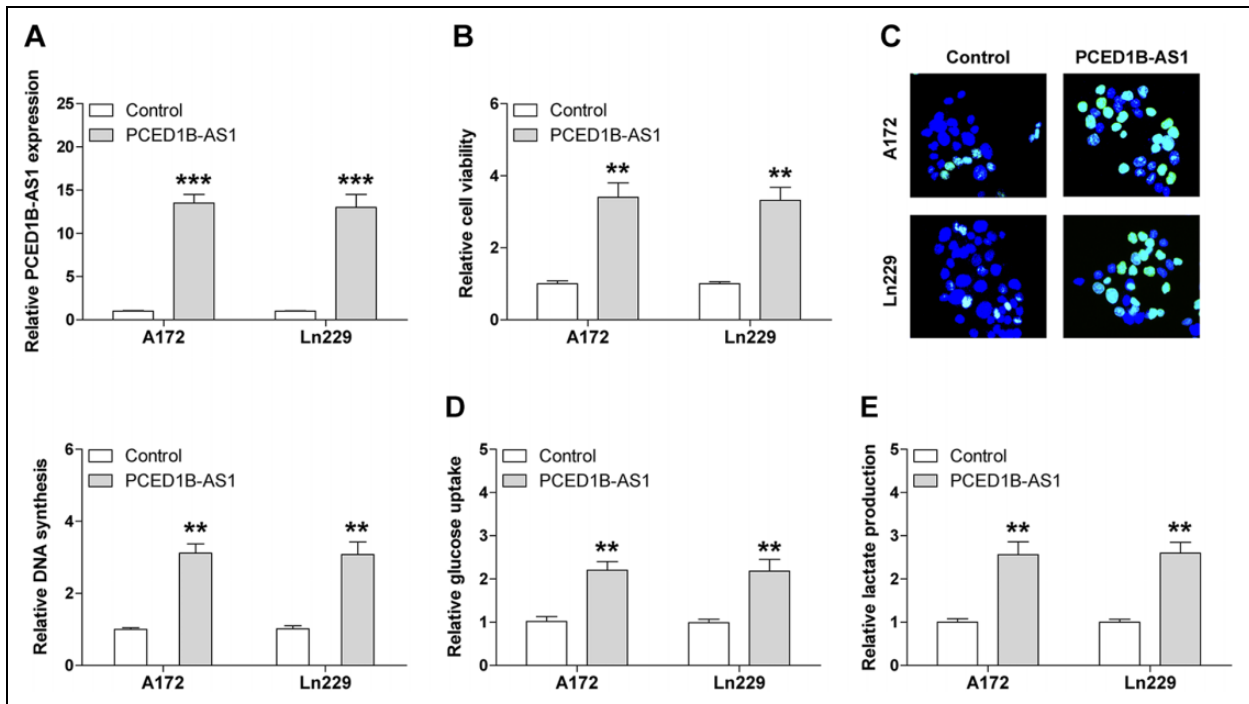


**Fig. 3.** PCED1B-AS1 overexpression promotes GBM cell proliferation, glucose uptake, and lactate release. (A) qRT-PCR analysis for verification of PCED1B-AS1 overexpression in A172 and Ln229 cell lines. (B) Cell viability in PCED1B-AS1-overexpressing A172 and Ln229 cell lines tested by CCK-8 assay. (C) DNA synthesis rate in PCED1B-AS1-overexpressing A172 and Ln229 cell lines detected by EdU assay. (D and E) The levels of glucose uptake and lactate release in A172 and Ln229 cell lines with or without PCED1B-AS1 overexpression. \*\* $P < 0.01$ , \*\*\* $P < 0.001$ . EdU: 5-Ethynyl-2'-deoxyuridine; GBM: glioblastoma; PCED1B-AS1: PCED1B antisense RNA I; qRT-PCR: quantitative reverse transcription polymerase chain reaction.

synthesized HIF-1 $\alpha$  protein, the lysates of U87MG and U251MG cells were collected after incubation with L-azido-homoalanine (Invitrogen) for 2.5 h. Then, the proteins were labeled using Click-iT Protein Reaction Buffer Kit (Invitrogen) as per the standard protocols, followed by incubation with streptavidin magnetic beads (Invitrogen). The enriched products were subjected to western blot analysis of HIF-1 $\alpha$  protein expression.

### RNA Pull-Down Assay

The biotinylated probes were *in vitro* transcribed using T7 High Yield RNA Synthesis Kit (Ambion, Austin, TX, USA) and labeled using RNA 3' End Biotinylation Kit (Thermo Fisher Scientific, Waltham, MA, USA) according to the manufacturer's instructions. Then, the above probes were incubated with whole-cell lysates of U87MG and U251MG cells at 4°C overnight, followed by addition with streptavidin magnetic beads (Invitrogen) and incubation at room temperature for 1 h with agitation. Finally, the RNA enrichment was analyzed by qRT-PCR.

### In Vivo Xenograft Assay

This animal experiment was carried out with the approval of the Animal Welfare Committee of The First Affiliated

Hospital of Zhengzhou University. A total of 15 BALB/c nude mice were obtained from Shanghai Experimental Animal Center, Chinese Academy of Sciences. They were randomly divided into three groups and subcutaneously injected with  $1 \times 10^7$  control or PCED1B-AS1-depleted U87MG cells, followed by growth under specific-pathogen-free condition for 5 weeks. At the end of the observation, all mice were euthanized by cervical dislocation and the tumors were weighed and collected for western blot and qRT-PCR analysis.

### Statistical Analysis

The difference between the two groups was statistically analyzed by Student's *t*-test or chi-square test according to the type of variables. One-way analysis of variance with Tukey honestly significant difference test was employed to assess the differences between multiple groups. The survival rate of GBM patients with high or low PCED1B-AS1 expression was compared using Kaplan–Meier plotter and analyzed by log-rank test. All results are the mean  $\pm$  SD of at least three independent experiments carried out in triplicate. The statistical significance was set to  $P < 0.05$ . All statistical analysis was performed using Graphpad Prism 7.0 software (Graphpad, San Diego, CA, USA).



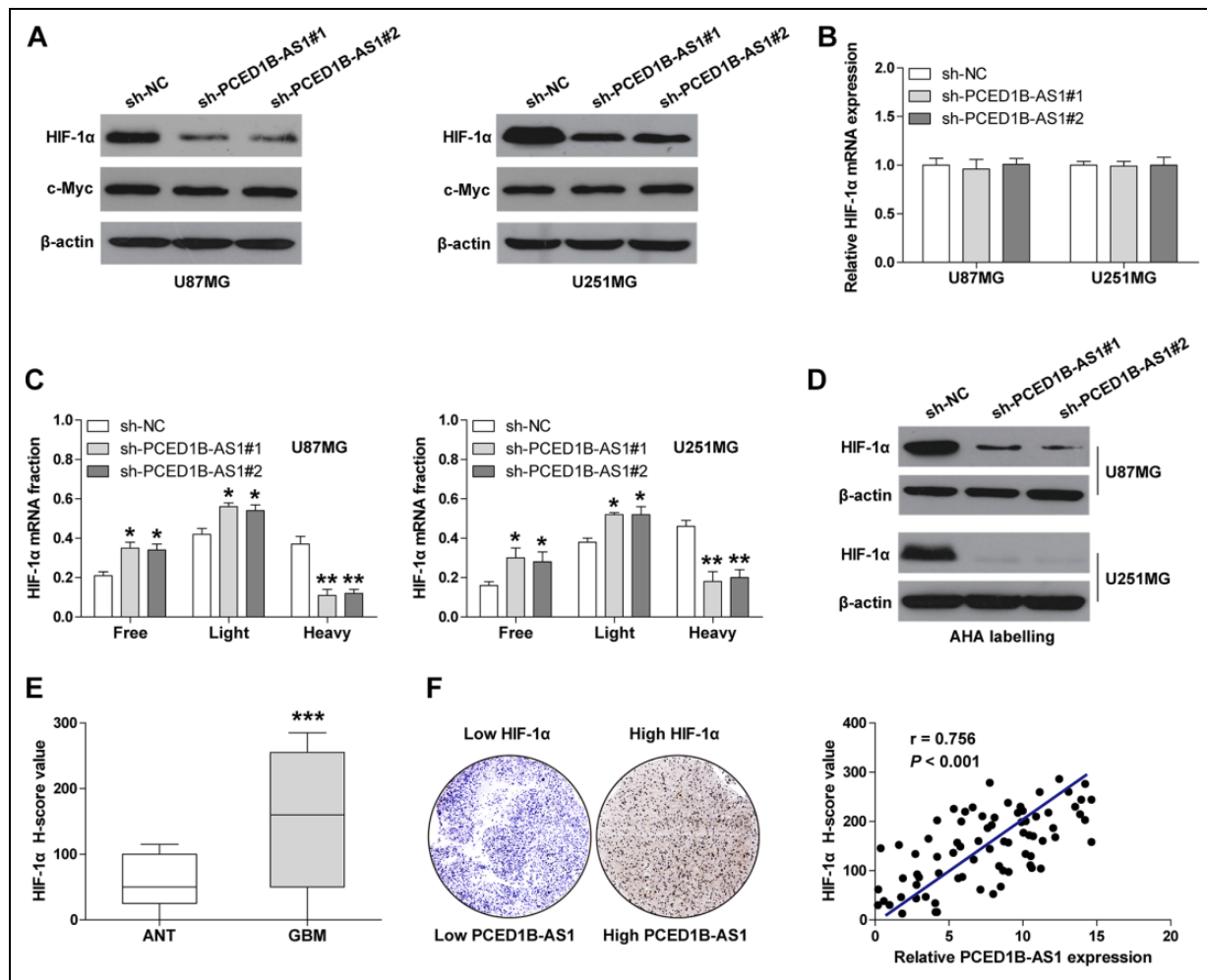


**Fig. 4.** PCED1B-AS1 upregulates HIF-1 $\alpha$  expression via promoting its translation process. (A) The protein expression of HIF-1 $\alpha$  and c-Myc in PCED1B-AS1-depleted U87MG and U251MG cell lines detected by western blot. (B) qRT-PCR analysis of HIF-1 $\alpha$  mRNA expression in PCED1B-AS1-depleted U87MG and U251MG cell lines. (C) qRT-PCR analysis of HIF-1 $\alpha$  mRNA level in the indicated polysome fractions of PCED1B-AS1-depleted U87MG and U251MG cell lines. (D) Western blot analysis of the newly synthesized HIF-1 $\alpha$  protein in PCED1B-AS1-depleted U87MG and U251MG cell lines. (E) IHC staining of HIF-1 $\alpha$  protein in GBM and normal tissues. (F) The correlation between PCED1B-AS1 and HIF-1 $\alpha$  protein in GBM tissues. \* $P < 0.05$ , \*\* $P < 0.01$ , \*\*\* $P < 0.001$ . AHA: L-azidohomoalanine; ANT: adjacent normal tissue; GBM: glioblastoma; PCED1B-AS1: PCED1B antisense RNA 1; qRT-PCR: quantitative reverse transcription polymerase chain reaction.

## Results

### Upregulation of PCED1B-AS1 Predicts Poor Prognosis for Patients with GBM

By analyzing the Gene Expression Profiling Interactive Analysis (GEPIA) database, we found that PCED1B-AS1 was the most upregulated lncRNA in GBM as compared with normal tissues (Fig. 1A). Then, we collected 76 paired GBM and paracancerous normal tissues to test the above result. As shown in Fig. 1B, PCED1B-AS1 was lowly expressed only in 7 (9%) cases. Also, PCED1B-AS1 was notably elevated in six GBM cell lines in comparison to normal NHA astrocyte cells (Fig. 1C). Next, we evaluated the relationship between PCED1B-AS1 expression and clinicopathological features of GBM patients. The results showed that high PCED1B-AS1

was positively correlated with larger tumor size and higher glioma grade (Table 1). More importantly, patients with high PCED1B-AS1 displayed shorter survival time than those with low PCED1B-AS1 (Fig. 1D). These data suggest that PCED1B-AS1 is upregulated in GBM and may be used as a potential prognostic indicator.

### Depletion of PCED1B-AS1 Represses the Warburg Effect and Proliferation of GBM Cells

To explore the biological function of PCED1B-AS1 in GBM, we established stable PCED1B-AS1 knockdown U87MG and U251MG cell lines by using the pCDH-CMV-MCS-EF1-copRFP lentiviral vector (Fig. 2A). As shown in Fig. 2B, the viability of U87MG and U251MG

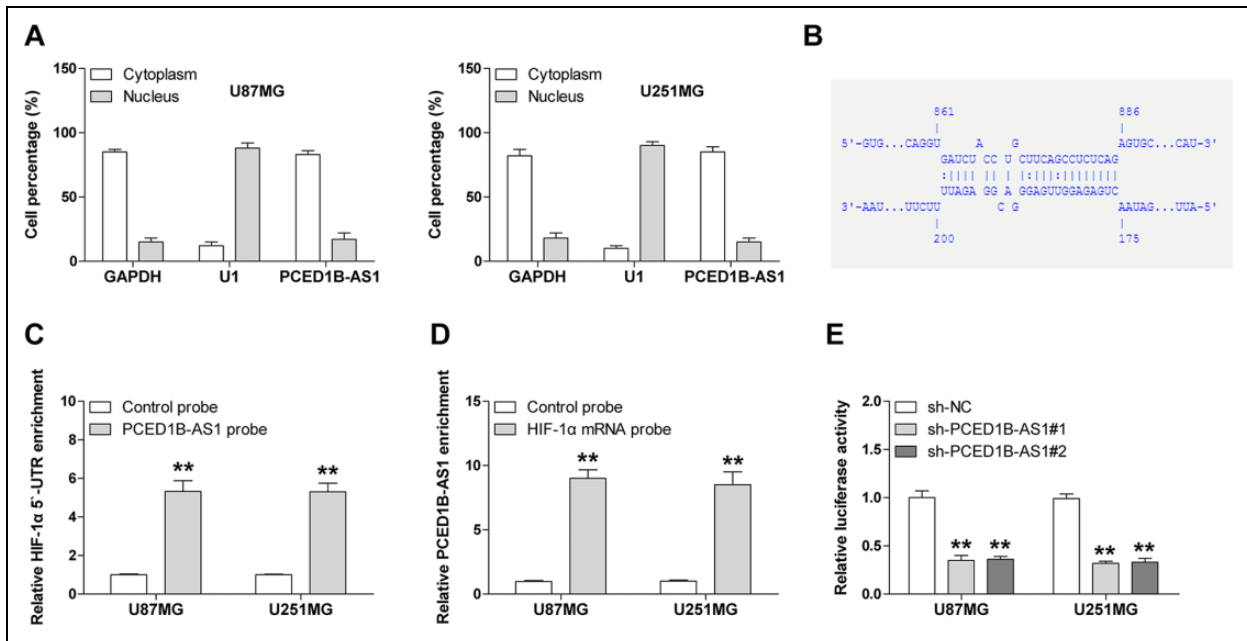


**Fig. 5.** PCED1B-AS1 directly binds to the 5'-UTR of HIF-1 $\alpha$  mRNA. (A) qRT-PCR analysis of the location of PCED1B-AS1 in U87MG and U251MG cell lines. GAPDH and UI were used as cytoplasmic and nuclear control references, respectively. (B) The interaction sequence of PCED1B-AS1 and 5'-UTR of HIF-1 $\alpha$  mRNA. (C and D) RNA pull-down coupled with qRT-PCR analysis in U87MG and U251MG cell lines using the indicated biotinylated probes. (E) The translation activity of 5'-UTR of HIF-1 $\alpha$  mRNA in U87MG and U251MG cell lines detected by luciferase reporter assay. \*\* $P < 0.01$ . GAPDH: glyceraldehyde-3-phosphate dehydrogenase; GBM: glioblastoma; PCED1B-AS1: PCED1B antisense RNA 1; qRT-PCR: quantitative reverse transcription polymerase chain reaction.

cells was drastically reduced after depletion of PCED1B-AS1. Similarly, less DNA synthesis was observed in PCED1B-AS1-silenced cells compared to control cells (Fig. 2C, D). Given that abnormal glucose metabolism is responsible for uncontrolled proliferation of cancer cells, we then tested the levels of glucose uptake and lactate production. The results showed that knockdown of PCED1B-AS1 significantly decreased the levels of glucose uptake (Fig. 2E) and lactate production (Fig. 2F) in both U87MG and U251MG cells. These functional assays indicate that PCED1B-AS1 knockdown inhibits GBM cell growth via blocking the Warburg effect.

### Overexpression of PCED1B-AS1 Potentiates the Warburg Effect and Proliferation of GBM Cells

We also established the PCED1B-AS1-overexpressing A172 and Ln229 cell lines. The overexpression efficiency was verified by qRT-PCR (Fig. 3A). In contrast, exogenous PCED1B-AS1 expression remarkably increased cell viability and DNA synthesis rate (Fig. 3B, C), as illustrated by CCK-8 and EdU assays, respectively. Likewise, more glucose uptake and lactate production were observed after enforced expression of PCED1B-AS1 in both A172 and Ln229 cells (Fig. 3D, E). These data further confirm the oncogenic role of PCED1B-AS1 in GBM.

### HIF-1 $\alpha$ Is a Downstream Target of PCED1B-AS1

In light of the pivotal regulatory role of HIF-1 $\alpha$  and c-Myc in the Warburg effect, we then tested whether PCED1B-AS1 functioned via them. As shown in Fig. 4A, knockdown of PCED1B-AS1 significantly reduced the protein expression levels of HIF-1 $\alpha$ , but not c-Myc. And HIF-1 $\alpha$  protein was uniformly overexpressed in GBM cells in comparison with normal NHA cells (supplemental Figure S1). However, PCED1B-AS1 did not affect HIF-1 $\alpha$  mRNA level (Fig. 4B), implying that PCED1B-AS1 controlled HIF-1 $\alpha$  expression at the post-transcriptional level. Subsequently, less HIF-1 $\alpha$  mRNA was observed in the heavy polysome fraction after PCED1B-AS1 knockdown (Fig. 4C), suggesting that PCED1B-AS1 promoted HIF-1 $\alpha$  mRNA translation. Consistently, depletion of PCED1B-AS1 resulted in a dramatic reduction in newly synthesized HIF-1 $\alpha$  protein in both U87MG and U251MG cells (Fig. 4D). In addition, we tested the expression of HIF-1 $\alpha$  protein in GBM tissues by IHC staining. The results showed that HIF-1 $\alpha$  protein expression was notably upregulated in GBM as compared with adjacent normal tissues (Fig. 4E), and its expression was strongly positively correlated with PCED1B-AS1 expression ( $r = 0.756$ ,  $P < 0.001$ ) (Fig. 4F). These results demonstrate that PCED1B-AS1 elevates HIF-1 $\alpha$  protein expression by facilitating HIF-1 $\alpha$  mRNA translation.

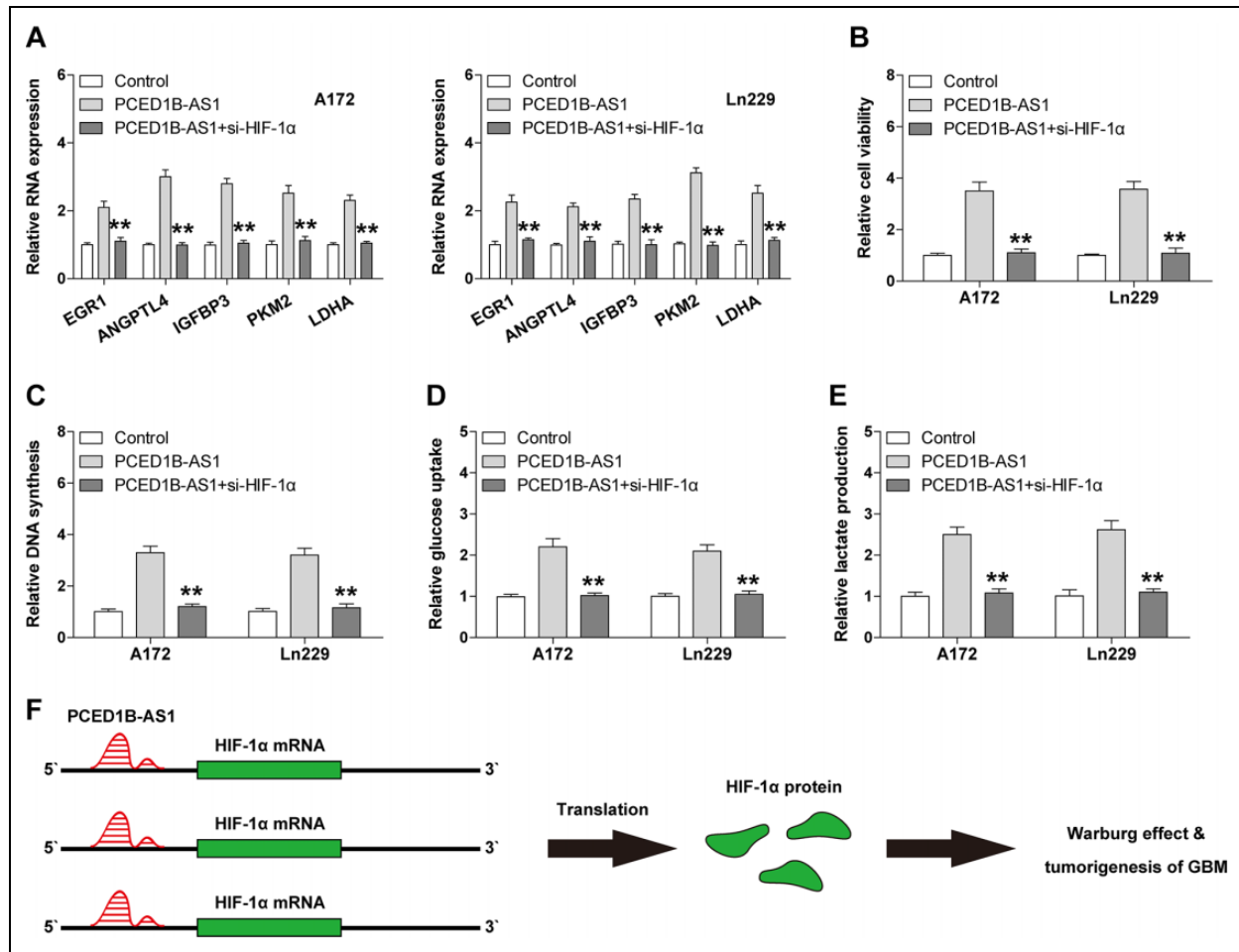


**Fig. 6.** HIF-1 $\alpha$  is required for the pro-oncogenic role of PCED1B-AS1. (A) qRT-PCR analysis of the indicated gene expression in PCED1B-AS1-overexpressing A172 and Ln229 cell lines transfected with HIF-1 $\alpha$  siRNA. (B) Cell viability in PCED1B-AS1-overexpressing A172 and Ln229 cell lines transfected with HIF-1 $\alpha$  siRNA detected by CCK-8 assay. (C) DNA synthesis rate in PCED1B-AS1-overexpressing A172 and Ln229 cell lines transfected with HIF-1 $\alpha$  siRNA detected by EdU assay. (D and E) The levels of glucose uptake and lactate release in PCED1B-AS1-overexpressing A172 and Ln229 cell lines transfected with HIF-1 $\alpha$  siRNA. (F) The proposed model of the pro-oncogenic role of PCED1B-AS1 via regulation of HIF-1 $\alpha$  translation in GBM. \*\* $P < 0.01$ . EdU: 5-Ethynyl-2'-deoxyuridine; GBM: glioblastoma; PCED1B-AS1: PCED1B antisense RNA 1; qRT-PCR: quantitative reverse transcription polymerase chain reaction.

### PCED1B-AS1 Directly Binds to the 5'-UTR of HIF-1 $\alpha$ mRNA

To determine how PCED1B-AS1 promotes HIF-1 $\alpha$  mRNA translation, we first tested the subcellular localization of PCED1B-AS1. As shown in Fig. 5A, PCED1B-AS1 was predominantly located in the cytoplasm, which was consistent with its role in posttranscriptional regulation of HIF-1 $\alpha$ . It has been well documented that lncRNA is able to govern gene expression by directly binding to DNA, RNA, or protein. Through sequence alignment, we found that PCED1B-AS1 might interact with the 5'-UTR of HIF-1 $\alpha$  mRNA (energy =  $-15.25480$  kcal/mol; Fig. 5B). To verify this possibility, we performed RNA pull-down assay coupled with qRT-PCR analysis. The results showed that more HIF-1 $\alpha$  5'-UTR/PCED1B-AS1 was enriched by PCED1B-AS1/HIF-1 $\alpha$  5'-UTR probes in comparison to control probes, respectively (Fig. 5C, D). In addition, the luciferase activity

of bicistronic reporter containing HIF-1 $\alpha$  5'-UTR was dramatically decreased in PCED1B-AS1-depleted U87MG and U251MG cells compared with control cells (Fig. 5E). These data indicate that PCED1B-AS1 accelerates HIF-1 $\alpha$  translation by physically interacting with the 5'-UTR of HIF-1 $\alpha$  mRNA.

### PCED1B-AS1 Functions in a HIF-1 $\alpha$ -Dependent Manner

We then tested the expression levels of HIF-1 $\alpha$  downstream targets after manipulating PCED1B-AS1 expression. The qRT-PCR results showed that ectopic expression of PCED1B-AS1 significantly elevated the expression of EGR1, ANGPTL4, IGFBP3, PKM2, and LDHA in both A172 and Ln229 cells, whereas these effects were evidently blocked by HIF-1 $\alpha$  silencing



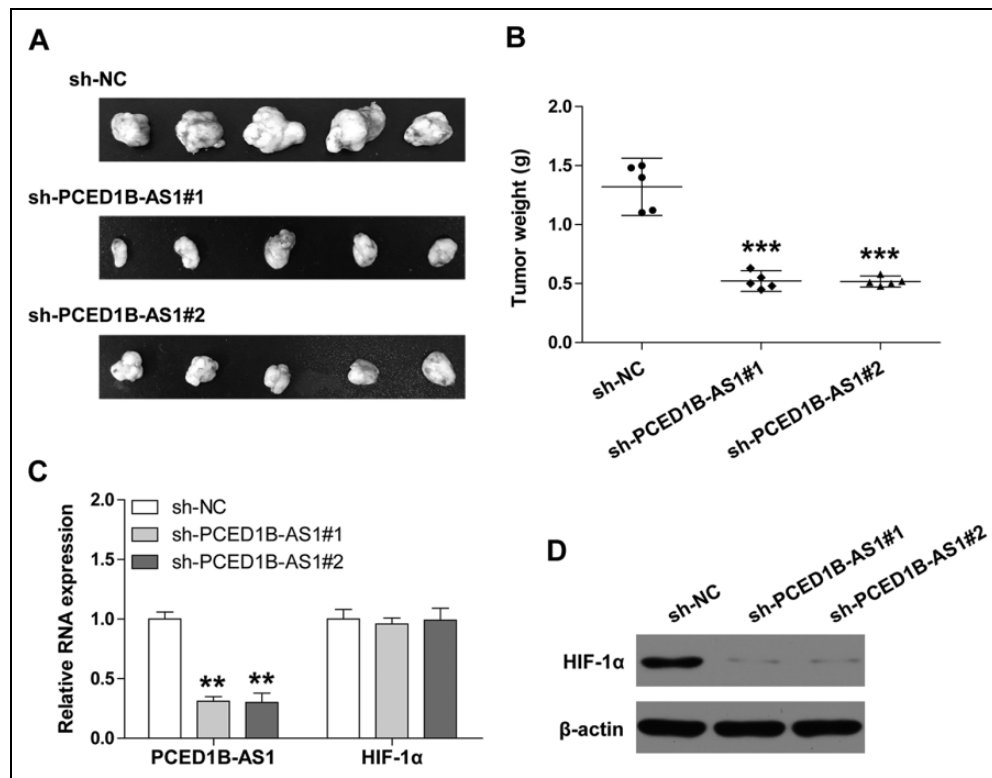


**Fig. 7.** Depletion of PCED1B-AS1 retards tumor growth. (A) The tumor images of nude mice in the indicated three groups ( $n = 5$  per group). (B) The tumor weights of nude mice in the indicated three groups. (C) qRT-PCR analysis of the expression of PCED1B-AS1 and HIF-1 $\alpha$  in the indicated three groups. (D) Western blot analysis of HIF-1 $\alpha$  protein expression in the indicated three groups;  $\beta$ -actin was used as loading control. \*\* $P < 0.01$ , \*\*\* $P < 0.001$ . PCED1B-AS1: PCED1B antisense RNA 1; qRT-PCR: quantitative reverse transcription polymerase chain reaction.

(Fig. 6A, supplemental Figure S2). Besides, exogenous PCED1B-AS1 expression enhanced cell viability, DNA synthesis, glucose uptake, and lactate production only in control cells, but not in HIF-1 $\alpha$ -depleted cells (Fig. 6B–E), implying that HIF-1 $\alpha$  is indispensable for the oncogenic role of PCED1B-AS1 (Fig. 6F).

#### Knockdown of PCED1B-AS1 Inhibits Tumor Growth

To test whether PCED1B-AS1 also functioned in vivo, we established the xenograft tumor model by subcutaneous injection of control or PCED1B-AS1-depleted cells into nude mice ( $n = 5$  in each group). Five weeks later, all mice were sacrificed and the results showed that the tumors in PCED1B-AS1-depleted groups were significantly smaller than those in control group (Fig. 7A, B). Likewise, knockdown of PCED1B-AS1 had no effect on HIF-1 $\alpha$  mRNA level (Fig. 7C). However, the protein levels of HIF-1 $\alpha$  were dramatically decreased in PCED1B-AS1-depleted groups in comparison to control group (Fig. 7D). These data suggest that PCED1B-AS1 knockdown retards tumor growth via downregulating HIF-1 $\alpha$  in vivo.

#### Discussion

In the present study, we described a novel GBM-related lncRNA, PCED1B-AS1, which was markedly overexpressed in GBM and closely correlated with aggressive clinical features and adverse prognosis. Loss- and gain-of-function assays indicated that knockdown of PCED1B-AS1 inhibited the Warburg effect and cell proliferation, while overexpression of PCED1B-AS1 resulted in opposite effects. Further mechanistic study revealed that HIF-1 $\alpha$  was a direct downstream target of PCED1B-AS1, in which PCED1B-AS1 was able to directly bind to the 5'-UTR of HIF-1 $\alpha$  mRNA, resulting in accelerated HIF-1 $\alpha$  translation, thereby elevating HIF-1 $\alpha$  protein expression and promoting the Warburg effect and tumorigenesis of GBM. In addition, we also observed a strong correlation between PCED1B-AS1 and HIF-1 $\alpha$  protein expression in GBM tissues and in the xenograft tumor model. Therefore, our data highlight the importance of PCED1B-AS1 in the progression of GBM and also shed new light on the regulation of lncRNA on protein translation.

lncRNA is emerging as a crucial player in the occurrence, development, and progression of cancer<sup>13</sup>. It can act as a tumor suppressor or an oncogene depending on the different contexts<sup>14</sup>. The mechanism by which lncRNA works is extremely complex, but accumulating evidence suggests that

this is closely related to its subcellular localization. Cytoplasmic lncRNA mainly functions via sponging miRNAs, binding to proteins and even translating peptides<sup>15</sup>. On the other hand, nuclear localized lncRNA is able to directly interact with epigenetic modification complex, influence chromatin architecture, and control gene expression at the transcriptional level<sup>16</sup>. Herein, we found that PCED1B-AS1 was mainly located in the cytoplasm, and it could directly bind to the 5'-UTR of HIF-1 $\alpha$  mRNA to potentiate HIF-1 $\alpha$  translation. To the best of our knowledge, only a few studies have focused on the direct binding of lncRNA to mRNA to affect its translation. For instance, lncRNA PXN-AS1 was reported to physically interact with the coding sequences of PXN mRNA, leading to dissociating the translation elongation factors from PXN mRNA and inhibiting its translation<sup>17</sup>. lncRNA NPCCAT1 was proposed as a translation promoter of YY1 by directly binding to the 5'-UTR of YY1 mRNA<sup>18</sup>. In this study, we hypothesize that PCED1B-AS1 may recruit some translation triggers (such as YB1<sup>19</sup>) by binding to HIF-1 $\alpha$  5'-UTR, thus promoting HIF-1 $\alpha$  translation, which requires further study.

HIF-1 $\alpha$  has been widely recognized as a key trigger of the Warburg effect that increases the expression of glycolysis genes by binding to hypoxia-responsive elements (HRE) on their promoters<sup>20</sup>. Dysfunctions of the regulatory system for HIF-1 $\alpha$  activity are critical for tumorigenesis<sup>21</sup>. A growing body of evidence has shown that HIF-1 $\alpha$  is significantly upregulated in various human cancers and predicted poor prognosis<sup>22</sup>. Up to now, several lncRNAs have been reported to be responsible for the dysregulation of HIF-1 $\alpha$ , such as TUG1<sup>23</sup>, MEG3<sup>24</sup>, PVT1<sup>25</sup>, and MTA2TR<sup>26</sup>. They controlled HIF-1 $\alpha$  expression by altering HIF-1 $\alpha$  mRNA levels, modulating the HIF-1 $\alpha$  translation process, or affecting HIF-1 $\alpha$  protein stability. Here, we confirmed that HIF-1 $\alpha$  protein was elevated in GBM tissues and found that PCED1B-AS1 promoted HIF-1 $\alpha$  protein expression, but not mRNA expression, by directly binding to the 5'-UTR of HIF-1 $\alpha$  mRNA and accelerating its translation process. Importantly, PCED1B-AS1 had no tumor-promoting effect in the absence of HIF-1 $\alpha$ , suggesting that PCED1B-AS1 functions in a HIF-1 $\alpha$ -dependent manner in GBM. Therefore, our study advances the understanding of the regulation of HIF-1 $\alpha$ , and meanwhile underlines the essential relevance of lncRNA in gene regulation. Intriguingly, we also found some HRE motifs on the promoter PCED1B-AS1. Whether a regulatory feed-forward loop was formed between PCED1B-AS1 and HIF-1 $\alpha$  to amplify the tumor-promoting effect of PCED1B-AS1 is worthy of in-depth investigation.

Of note, by analyzing the GEPIA database, we found that PCED1B-AS1 was also upregulated in several human cancers, such as diffuse large B cell lymphoma and kidney renal clear cell carcinoma, as shown in supplemental Figure S3. Further study is needed to confirm this observation to expand the clinical implication of PCED1B-AS1.

Collectively, our findings for the first time demonstrate that PCED1B-AS1 is a pro-oncogenic lncRNA in GBM

through regulation of HIF-1 $\alpha$  mRNA translation. Targeting this regulatory axis of PCED1B-AS1/HIF-1 $\alpha$  may be a promising approach for the treatment of GBM patients.

### Ethical Approval

Ethical approval to report this case series was obtained from the Ethics Committee of The First Affiliated Hospital of Zhengzhou University.

### Statement of Human and Animal Rights

All procedures involving the care and use of laboratory animals were approved by the Animal Policy and Welfare Committee of The First Affiliated Hospital of Zhengzhou University, and all efforts were made to minimize use of animals as well as to minimize their pain or discomfort during the course of the study.

### Statement of Informed Consent

Written informed consent was obtained from the patients for their anonymized information to be published in this article.


### Declaration of Conflicting Interests

The author(s) declared no potential conflicts of interest with respect to the research, authorship, and/or publication of this article.

### Funding

The author(s) disclosed receipt of the following financial support for the research, authorship, and/or publication of this article: This work was supported by grant from Post-doctoral Science Foundation Project (No. 61).

### ORCID iD

Xianzhi Liu  <https://orcid.org/0000-0003-3965-1815>

### Supplemental Material

Supplemental material for this article is available online.

### References

1. Wirsching HG, Galanis E, Weller M. Glioblastoma. *Handb Clin Neurol*. 2016;134:381–397.
2. Alexander BM, Cloughesy TF. Adult glioblastoma. *J Clin Oncol*. 2017;35(21):2402–2409.
3. Batash R, Asna N, Schaffer P, Francis N, Schaffer M. Glioblastoma multiforme, diagnosis and treatment; recent literature review. *Curr Med Chem*. 2017;24(27):3002–3009.
4. Ostrom QT, Gittleman H, Liao P, Rouse C, Chen Y, Dowling J, Wolinsky Y, Kruchko C, Barnholtz-Sloan J. CBTRUS statistical report: primary brain and central nervous system tumors diagnosed in the united States in 2007-2011. *Neuro Oncol*. 2014;16(Suppl 4):v1–v63.
5. Pavlova NN, Thompson CB. The emerging hallmarks of cancer metabolism. *Cell Metab*. 2016;23(1):27–47.
6. Liberti MV, Locasale JW. The Warburg effect: how does it benefit cancer cells? *Trends Biochem Sci*. 2016;41(3):211–218.
7. Strickaert A, Saiselet M, Dom G, De Deken X, Dumont JE, Feron O, Sonveaux P, Maenhaut C. Cancer heterogeneity is not

- compatible with one unique cancer cell metabolic map. *Oncogene*. 2017;36(19):2637–2642.
8. San-Millan I, Brooks GA. Reexamining cancer metabolism: lactate production for carcinogenesis could be the purpose and explanation of the Warburg Effect. *Carcinogenesis*. 2017;38(2):119–133.
  9. Yang F, Zhang H, Mei Y, Wu M. Reciprocal regulation of HIF-1alpha and lincRNA-p21 modulates the Warburg effect. *Mol Cell*. 2014;53(1):88–100.
  10. Xiang S, Gu H, Jin L, Thorne RF, Zhang XD, Wu M. LncRNA IDH1-AS1 links the functions of c-Myc and HIF1alpha via IDH1 to regulate the Warburg effect. *Proc Natl Acad Sci USA*. 2018;115(7):E1465–E1474.
  11. Luo F, Liu X, Ling M, Lu L, Shi L, Lu X, Li J, Zhang A, Liu Q. The lncRNA MALAT1, acting through HIF-1alpha stabilization, enhances arsenite-induced glycolysis in human hepatic L-02 cells. *Biochim Biophys Acta*. 2016;1862(9):1685–1695.
  12. Zeng K, Chen X, Hu X, Liu X, Xu T, Sun H, Pan Y, He B, Wang S. LACTB, a novel epigenetic silenced tumor suppressor, inhibits colorectal cancer progression by attenuating MDM2-mediated p53 ubiquitination and degradation. *Oncogene*. 2018;37(41):5534–5551.
  13. Peng WX, Koirala P, Mo YY. LncRNA-mediated regulation of cell signaling in cancer. *Oncogene*. 2017;36(41):5661–5667.
  14. Ma L, Bajic VB, Zhang Z. On the classification of long non-coding RNAs. *RNA Biol*. 2013;10(6):925–933.
  15. Noh JH, Kim KM, McClusky WG, Abdelmohsen K, Gorospe M. Cytoplasmic functions of long noncoding RNAs. *Wiley Interdiscip Rev RNA*. 2018;9(3): e1471.
  16. Sun Q, Hao Q, Prasanth KV. Nuclear long noncoding RNAs: key regulators of gene expression. *Trends Genet*. 2018;34(2):142–157.
  17. Yuan JH, Liu XN, Wang TT, Pan W, Tao QF, Zhou WP, Wang F, Sun SH. The MBNL3 splicing factor promotes hepatocellular carcinoma by increasing PXN expression through the alternative splicing of lincRNA-PXN-AS1. *Nat Cell Biol*. 2017;19(7):820–832.
  18. Su H, Liu L, Zhang Y, Wang J, Zhao Y. Long noncoding RNA NPCCAT1 promotes nasopharyngeal carcinoma progression via upregulating YY1. *Biochimie*. 2019;157:184–194.
  19. El-Naggar AM, Veinotte CJ, Cheng H, Grunewald TG, Negri GL, Somasekharan SP, Corkery DP, Tirode F, Mathers J, Khan D, Kyle AH, et al. Translational activation of HIF1alpha by YB-1 promotes sarcoma metastasis. *Cancer Cell*. 2015;27(5):682–697.
  20. Goodwin ML, Gladden LB, Nijsten MW, Jones KB. Lactate and cancer: revisiting the Warburg effect in an era of lactate shuttling. *Front Nutr*. 2014;1:27.
  21. Brocato J, Chervona Y, Costa M. Molecular responses to hypoxia-inducible factor 1alpha and beyond. *Mol Pharmacol*. 2014;85(5):651–657.
  22. Hayashi Y, Yokota A, Harada H, Huang G. Hypoxia/pseudohypoxia-mediated activation of hypoxia-inducible factor-1alpha in cancer. *Cancer Sci*. 2019;110(5):1510–1517.
  23. Yu X, Hu L, Li S, Shen J, Wang D, Xu R, Yang H. Long non-coding RNA Taurine upregulated gene 1 promotes osteosarcoma cell metastasis by mediating HIF-1alpha via miR-143-5p. *Cell Death Dis*. 2019;10(4):280.
  24. Zhou C, Huang C, Wang J, Huang H, Li J, Xie Q, Liu Y, Zhu J, Li Y, Zhang D, Zhu Q, et al. LncRNA MEG3 downregulation mediated by DNMT3b contributes to nickel malignant transformation of human bronchial epithelial cells via modulating PHLPP1 transcription and HIF-1alpha translation. *Oncogene*. 2017;36(27):3878–3889.
  25. Wang Y, Chen W, Lian J, Zhang H, Yu B, Zhang M, Wei F, Wu J, Jiang J, Jia Y, Mo F, et al. The lncRNA PVT1 regulates nasopharyngeal carcinoma cell proliferation via activating the KAT2A acetyltransferase and stabilizing HIF-1alpha. *Cell Death Differ*. 2020;27(11):695–710.
  26. Zeng Z, Xu FY, Zheng H, Cheng P, Chen QY, Ye Z, Zhong JX, Deng SJ, Liu ML, Huang K, Li Q, et al. LncRNA-MTA2TR functions as a promoter in pancreatic cancer via driving deacetylation-dependent accumulation of HIF-1alpha. *Theranostics*. 2019;9(18):5298–5314.